Published in final edited form as:
Invest Ophthalmol Vis Sci. 2009 May ; 50(5): 2351–2358. doi:10.1167/iovs.08-2918.

Retinal Ion Regulation in a Mouse Model of Diabetic Retinopathy: Natural History and the Effect of Cu/Zn Superoxide Dismutase Overexpression

Bruce A. Berkowitz[1,2], **Marius Gradianu**[1], **David Bissig**[1], **Timothy S. Kern**[3], and **Robin Roberts**[1]

1*Department of Anatomy and Cell Biology, Wayne State University, Detroit, Michigan*

2*Department of Ophthalmology, Wayne State University, Detroit, Michigan*

3*Department of Department of Medicine, Case Western Reserve University, Cleveland, Ohio.*

Abstract

Purpose—To test the hypotheses that manganese-enhanced MRI (MEMRI) is useful in evaluating intraretinal ion dysregulation in wild-type (WT) and Cu/Zn superoxide dismutase (SOD1) overexpressor mice.

Methods—Central intraretinal ion activity and retinal thickness were measured from high-resolution data of light- and dark-adapted WT C57BL/6 mice (to gauge MEMRI sensitivity to normal visual processing in mice) and dark-adapted diabetic and nondiabetic WT and Cu/Zn superoxide dismutase overexpressor (SOD1OE) mice. Glycated hemoglobin and retinal vascular histopathology were also determined.

Results—In WT mice, light adaptation reduced outer retinal manganese uptake compared with that in dark adaptation; no effect on inner retinal uptake was found. In diabetic WT mice, intraretinal manganese uptake became subnormal between 1.5 and 4 months of diabetes onset and then relatively increased. Central retinal thickness, as determined with MEMRI, decreased as a function of age in diabetic mice but remained constant in control mice. Nondiabetic SOD1OE mice had normal retinal manganese uptake but subnormal retinal thickness and supernormal acellular capillary density. At 4.2 months of diabetes, SOD1OE mice had normal manganese uptake and no further thinning; acellular capillaries frequency did not increase by 9 to 10 months of diabetes.

Conclusions—In emerging diabetic retinopathy, MEMRI provided an analytic measure of an ionic dysregulatory pattern that was sensitive to SOD1 overexpression. The potential benefit of SOD1 overexpression to inhibit retinal abnormality in this model is limited by the retinal and vascular degeneration that develops independently of diabetes.

Microvascular abnormality is the clinical hallmark of diabetic retinopathy. Yet functional losses occur in the retina between the onset of hyperglycemia and the appearance of ophthalmoscopically visible microangiopathy. In this period of emergent diabetic retinopathy, dysfunction occurs not only in vascular retina (e.g., autoregulatory impairment) but also in nonvascular retina (e.g., reduced contrast sensitivity, relatively lower retinal electrophysiological parameters, and subnormal ion regulation).[1–16] The importance of such

Corresponding author: Bruce A. Berkowitz, Department of Anatomy and Cell Biology, Wayne State University School of Medicine, 540 E. Canfield, Detroit, MI 48201; E-mail: baberko@med.wayne.edu..

Disclosure: **B.A. Berkowitz**, None; **M. Gradianu**, None; **D. Bissig**, None; **T.S. Kern**, None; **R. Roberts**, None

functional impairment is underscored by noting that correction of early diabetes-induced retinal dysfunctionality, such as abnormal ion regulation, is linked to the inhibition of late-stage vascular histopathology.[17–19] For example, in experimental diabetes, preventive pharmaceutical treatment with captopril can inhibit early reductions in a major regulator of ion homeostasis in the retina, Na/K-ATPase activity, and can ameliorate late-stage development of vascular histopathology.[18,19] These associations are suggestive, and more work is needed to better define the factors regulating diabetes-induced subnormal retinal ion activity.

Pathobiochemical insults, such as oxidative stress, are also strongly linked with developing diabetic retinopathy. However, few studies have investigated the interplay between early diabetes-induced ion dysregulation and oxidative stress. Treating diabetic rats with α-lipoic acid corrected diabetes-induced reductions in retinal antioxidants such as manganese superoxide dismutase (SOD2) and Cu/Zn superoxide dismutase (SOD1).[20,21] The same treatment inhibited early ion dysregulation and late-stage vascular histopathology such as the degeneration of retinal capillaries.[17] Recent elegant work involving SOD2 overexpressor mice has established an important role of SOD2 in diabetic retinopathy.[20,22,23] SOD1 constitutes at least 85% of the total cellular superoxide dismutase activity in many mammalian cells, has high activity in the retina, and is a key defense against superoxide-related oxidative stress in the cytosol and intermembrane space of mitochondria.[24–26] Efforts to understand the role of SOD1 in nondiabetic models of retinal injury using SOD1 overexpressor mice have produced mixed results, with overexpression either increasing retinal neuronal damage, providing neuroprotection, or having no effect.[27–29] Despite strong evidence that diabetes causes an environment of early oxidative stress in retinas of rats and mice[23,30–32] and that antioxidant therapy inhibits the later degeneration of the retinal capillaries, a specific role of SOD1 in the diabetic retina has not been well studied.

One powerful noninvasive method for studying cellular ionic activity is manganese-enhanced MRI (MEMRI).[33,34] MEMRI allows for noninvasive measurement of retinal thickness and, notably, layer-specific uptake of manganese (Mn^{2+}) ion after systemic $MnCl_2$ injection.[17,35–37] Manganese ion, an MRI contrast agent and analog of, for example, calcium, readily accumulates intracellularly as a function of membrane integrity and cellular activity, is sensitive to Na/K-ATPase activity, and is relatively slowly removed.[33,35,38–40] In rat models of diabetic retinopathy and in a nondiabetic rat ischemia/reperfusion model that produces histopathology similar to that of diabetic retinopathy, impaired ion regulation developed before the appearance of neuronal and vascular degeneration.[17,35–37] Such changes in retinal ion regulation in mouse models of diabetic retinopathy have not yet been reported.

In this study, we evaluated the sensitivity of MEMRI to normal changes in retinal ion regulation with light and dark adaption (i.e., visual processing) in the mouse retina in vivo. Next, we described the natural history of MEMRI changes before and during the appearance of acellular capillaries in mice. In addition, we compared the effect of diabetes in wild-type (WT) mice and transgenic mice that overexpress SOD1 on intraretinal ion regulation and thickness and on vascular histopathology. If increased oxidative stress played an important role in altering ion homeostasis in diabetic retinopathy, the upregulation of SOD1 activity would have been expected to be protective against early ion dysregulation and, possibly, late-stage histopathology.[29]

Methods

Animals were treated in accordance with the Principles of Laboratory Animal Care (National Institutes of Health publication no. 85−23, revised 1985; http://grants1.nih.gov/grants/olaw/references/phspol.htm) and with the ARVO Statement for the Use of Animals in Ophthalmic and Vision Research. MRI is ideally suited for studying the

same animal over time, and a single injection of manganese is nontoxic (vide infra). Because of the slow clearance of manganese from the body at this time, however, repeated dosing may be reasonable every 3 months or so (though much shorter repeat times are possible; the studies investigating this have not yet been performed). For these reasons, we chose to investigate different animals at different ages to improve our time resolution.

Groups

For visual processing comparisons, different groups of female C57BL/6 mice (WT; $n = 4$ per condition; average age, 3 months; Hilltop Laboratory Animals, Inc., Scottdale, PA) were studied using a light- and dark-adaptation procedure previously described in rats.[39] Natural history studies were conducted in dark-adapted animals with the following male C57BL/6 groups that were diabetic (chronologic age/diabetes duration): 3.6 months/0.9 months, $n = 5$; 4.1 month/1.5 months, $n = 5$; 5.2 months/2.5 months, $n = 6$; 8.2 months/5.5 months, $n = 6$; 10 months/7.4 months, $n = 4$ (The Jackson Laboratory, Bar Harbor, ME). An additional dark-adapted group (C57BL/6 mice from Hilltop Animals, Inc.) was also studied: 7.2 months/4 months, $n = 5$. Nondiabetic control mice were also examined: chronologic age: 3.3 months, $n = 7$; 4.9 months, $n = 5$; 8 months, $n = 3$ (The Jackson Laboratory), or 7.4 months, $n = 6$ (Hilltop Laboratory Animals, Inc.). The effect of SOD1 overexpression was examined in the following two groups of dark-adapted C57BL/6 mice: SOD1OE control (SOD1OE, $n = 4$ males; average age, 5 months; The Jackson Laboratory) and diabetic male SOD1 overexpressor mice (SOD1OE+D, $n = 4$ males; average age, 7.1 months; diabetic, 4.2 months; The Jackson Laboratory). SOD1OE mice have a twofold to threefold increase in central nervous system SOD1 activity[41,42] (http://jaxmice.jax.org/strain/002629rf.html). Importantly, it has been reported that diabetes had no effect on the extent of SOD1 overexpression.[41]

Diabetes was induced in mice with starting weights of 20 to 24 g by streptozotocin (60 mg/kg; 10 mM citrate buffer [pH 4.5]) intraperitoneal injection once a day for 5 consecutive days. Body weight and blood glucose levels were monitored weekly. Insulin (neutral protamine Hagedorn) was administered to allow slow weight gain while maintaining hyperglycemia (blood glucose levels higher than 400 mg/dL). Normal rodent chow and water were provided ad libitum. All mice were housed in normal 12-hour cycled laboratory lighting until the end of the experiment. Glycated hemoglobin was measured from blood collected after each MEMRI experiment (Glyco-Tek affinity columns, kit 5351; Helena Laboratories, Beaumont, TX). After 4 months of diabetes, only mice with blood glucose levels higher than 400 mg/dL were studied through MEMRI.

High-Resolution MRI

All mice were maintained in darkness for 16 to 20 hours before manganese injection. Procedures (e.g., weighing, injecting $MnCl_2$, anesthetic administration, and MRI examination) were performed under dim red light or darkness. $MnCl_2$ was administered as an intraperitoneal injection (66 mg/kg) on the right side of awake mice. After this injection, mice were maintained in dark conditions for another 3.5 to 4 hours. Immediately before the MRI experiment, mice were anesthetized with urethane (36% solution intraperitoneally; 0.083 mL/20 g animal weight, prepared fresh daily; Aldrich, Milwaukee, WI) and xylazine (1−8 mg/kg intraperitoneally). Urethane alone tended to increase the respiratory frequency of the mice and thus motion artifacts on MEMRI. The addition of a small amount of the muscle relaxant xylazine minimized these artifacts. Core temperatures were maintained with a recirculating heated water blanket. MRI data were acquired on a 4.7-T system (Avance; Bruker) with a two-turn transmit/receive surface coil (1.0-cm diameter) placed over the left eye. A single transverse slice through the center of the eye (based on sagittal localizer images collected with the same adiabatic pulse sequence as described) was obtained for each mouse. Transverse images were then acquired using an adiabatic spin-echo imaging sequence (repetition time, 350 seconds; echo time, 16.7

ms; number of acquisitions, 16; sweep width, 61,728 Hz; matrix size, 512 × 512; slice thickness, 620 μm; pixel size, 23.4 × 23.4 × 620 μm^3; field of view, 12 × 12 mm^2).[43] After the MEMRI examination, a final blood sample was obtained for glycated hemoglobin analysis, and mice were humanely euthanized.

Histopathology

A separate batch of nondiabetic and diabetic SOD1OE mice, made diabetic simultaneously with those studied by MEMRI, were sent to the laboratory of one of the authors (TSK) and kept until 9 to 10 months of age before histopathologic examination. Age-matched WT control mice were maintained during this same time period and were used for comparison. Retinal vasculature was isolated by the trypsin digest method, as described previously.[44,45] Briefly, freshly isolated eyes were fixed with buffered formalin (4% [wt/vol] formaldehyde, 0.075 M sodium phosphate buffer). Retinas were isolated, washed in water overnight, and incubated with 3% crude trypsin (Difco; Becton Dickinson, Sparks, MD) at 37°C for 1 hour. Nonvascular cells were gently brushed away from the vasculature, and the isolated vasculature was mounted on glass slides, air dried, and stained with periodic acid-Schiff and hematoxylin.

Data Analysis

Layer-Specific Signal Intensity—For visualization purposes, software written in-house was used to map the in situ image into a linear representation for each retina. Within each group, linearized retinas were averaged into a composite image. For quantitative analysis, signal intensities were first extracted from each mouse image with the ImageJ program (developed by Wayne Rasband, National Institutes of Health, Bethesda, MD; available at http://rsb.info.nih.gov/ij/index.html.) and derived macros,[46] and the results from that group were compared with those of a generalized estimating equation approach.[39] Changes in receiver gain between animals were controlled for by setting the signal intensity of a fixed region of noise in each mouse to a fixed value. Other tissues within the sensitive volume of the coil may also be affected by diabetes with differential enhancement after manganese injection and so were considered inadequate as internal references. Postreceptor (or inner retina) and receptor (or outer retina) signal intensity data (from distances ±0.4 to 1 mm from the optic nerve) were extracted as follows: the inner/outer retinal division was observable in light-adapted retinas (based on contrast generated by the differential amount of manganese taken up in inner and outer retina) but was not observable in dark-adapted retinas (Fig. 1).[39] Thus, we took advantage of the fact that whole retina thickness values were within normal range for mice and assumed that the divisions between inner and outer retina and between retina and choroid occur as they do in normal retina, approximately 100 μm from the vitreal-retinal border or approximately 4 pixels, (23.4 × 4 = 96 μm) for inner retina and then 3 pixels posterior to this region to sample the outer retina. To further ensure that we measured from the inner and outer retina, the pixel values anterior each of these divisions were designated as representative of inner or outer retinal values, respectively. These regions are illustrated in Figure 1. Data were analyzed as previously described.[39]

In Hilltop animals, no difference ($P > 0.05$) in extent of manganese uptake in inner retina after dark adaptation was found between male (80.5 ± 1.2 [SEM] arbitrary units [AU]; $n = 6$) and female (84.1 ± 1.1 AU; $n = 4$) mice, and these data were combined for further comparisons.

Extraocular Muscle Signal Intensity—To assess a possible role for differences in systemic handling of manganese, the mean signal intensity for each mouse was measured from a fixed-size, ellipse-shaped region of interest drawn in the anterior-most aspect of the inferior rectus muscle. Mice that did not have a recognizable rectus muscle because of head and slice orientation were not included in the analysis of extraocular muscle. Extraocular muscle signal intensities from diabetic and control Hilltop mice were, respectively, 14% to 27% lower ($P <$

0.05) than those from Jackson Laboratory mice (data not shown), suggesting that differences in inner retinal uptake might be secondary to differences in systemic handling of manganese. Retinal measurements made in the same set of physiological conditions and in the same retinal layer (i.e., inner retina of similarly aged dark adaptation in control mice from both vendors) revealed that the signal intensities of Hilltop mice (81.9 ± 0.8 AU; $n = 10$) were 11% lower ($P < 0.05$) than of Jackson mice (90.8 ± 0.8 AU; $n = 12$). Thus, intraretinal data from all Hilltop mice (controls and diabetics) were scaled by multiplying by 1.11 (hereafter called modified Hilltop data) to allow for comparisons with the data of Jackson mice. The reason for the vendor difference is not clear but may represent a combination of differences in the genetics of the founder mice and genetic drift within each colony. In addition, we note that in a previous study in nondiabetic rats, simply reducing the injected dose of $MnCl_2$ by a factor of 2.9 (from 44 to 15 mg/kg) did not result in a decrease ($P > 0.05$) in intraretinal signal intensity 4 hours after injection (data not shown). Thus, the present vendor differences may reflect variations in organ or metabolic handling of manganese and not simply differences in plasma manganese levels. In any event, straightforward tissue-specific scalar normalization was adequate for removing these vendor-specific variations.

Retinal Thickness—Whole retinal thicknesses were determined from each MEMRI-generated image as the radial distance between the anterior edge and the posterior edge of the retina at distances ±0.4 to 1 mm from the optic nerve, as previously described.[47] Briefly, software written in-house was used to map the in situ image into a linear representation for each retina. Thicknesses were derived from these linearized images. First, the average signal intensity profile as a function of depth into the retina was determined by the program. Then the point at which the signal intensity profile crossed the average of the highest and lowest signal intensity near provisional vitreous/retina and retina/choroid+sclera boundaries was calculated automatically. The distance between these two midpoints was considered the whole retinal thickness. No difference was noted when automatically derived whole retinal thicknesses were compared with manually derived thickness (data not shown). Mean superior and inferior retinal values generated for each animal group were combined and used for comparisons.

Histopathology—Acellular capillaries were quantitated in six to eight field areas in the midretina (400× magnification) in a masked manner. Acellular capillaries were identified as capillary-sized vessel tubes with no nuclei anywhere along their lengths and were reported per square millimeter of retinal area. Tubes with diameters less than 30% of the diameter of adjacent capillaries were identified as strands and were not counted as acellular capillaries. Acellular capillaries for animals from all four groups were measured by the same reader (TSK) at the same time and in a masked manner.

Statistical Analysis

Comparisons of MEMRI retinal signal intensities were performed with a generalized estimating equation (GEE) approach.[39,48] GEE performs a general linear regression analysis using all the pixels in each subject and accounts for the within-subject correlation between adjacent pixels. An ANOVA-type GEE test is not readily available. Instead exact *P* values from two-tailed comparisons are provided. When the *P* values are very low (e.g., $P = 0.0001$), the likelihood of false rejection of a true null in multiple comparisons is very small.

Body weight, glycated hemoglobin, or retinal thickness data within and between WT control or diabetic groups were compared with the use of a nonparametric (because some groups only had three or four data points) Kruskal-Wallis ANOVA. Further analysis of these data, using a 2 × 2 ANOVA test or, if group variances were dissimilar, Bonferroni-corrected multiple *t*-tests, produced outcomes similar to those of Kruskal-Wallis ANOVA (data not shown). Histology

data were analyzed by the nonparametric Kruskal-Wallis test and then by the Mann-Whitney *U* test. Data are presented as mean ± SEM.

Results

Systemic Physiology

During the study, WT control mice (combined Jackson and modified Hilltop; see Methods) had constant body weights (range, 26−33 g; $P > 0.05$) or glycated hemoglobin levels (5.2% −5.8%; $P > 0.05$). Further comparisons were performed using the average WT body weight of 29.4 ± 0.5 g and glycated hemoglobin level of 5.7% ± 0.1% ($n = 21$; mean ± SEM). Within the WT diabetic group (all ages and vendors), similar body weights (24.6−26.4 g; $P > 0.05$) and glycated hemoglobin levels (10.6%−13.9%, $P > 0.05$) were found, but both parameters were different ($P < 0.05$) from the average WT values. Body weights of the SOD1OE (27.4 ± 1.5 g) and SOD1OE+D (24.8 ± 1.0 g) groups were not different ($P > 0.05$) from each other or from those of the WT controls. Glycated hemoglobin levels for SOD1OE mice (5.1% ± 0.2%) were not different from those of controls ($P > 0.05$), but those of the SOD1OE+D group (10.9% ± 0.7%) were.

MEMRI

Effect of Light Adaptation—In WT mice (modified Hilltop; see Methods for explanation), light- and dark-adapted retinas had similar ($P > 0.05$) inner retinal signal intensities but different ($P = 0.0025$) outer retinal intensities (Fig. 1).

Effect of Diabetes—In nondiabetic WT mice between 3.5 and 8 months of age, no significant differences ($P > 0.05$) were noted in signal intensity of inner (87.6−95.3 AU) or outer (86.1−93.1 AU) retina. Thus, average WT signal intensity for inner ($n = 21$; 91.1 ± 0.6 AU) and outer (89.2 ± 0.6 AU) retina were used for comparison with the diabetic data of similarly aged mice.

At 0.9 and 5.5 months of diabetes (chronological ages, 3.5 and 8.2 months), the degree of manganese uptake in inner and outer retina was not different from the average WT values ($P > 0.05$); no age-matched controls were available for comparisons with the 7.4-month diabetic (10-month chorological age) data (Fig. 2). Between 1.5 and 4 months of diabetes, the extent of inner and outer retinal uptake was similarly subnormal ($P = 0.0001$ at all time points). Compared with the combined 1.5- to 4-month diabetic data, intraretinal signal intensities were relatively increased at 0.9 months of diabetes ($P = 0.02$ [inner retina]; $P = 0.05$ [OR]), and 5.5 and 7.4 months of diabetes ($P = 0.0001$ at each time point).

To investigate the possibility that systemic alterations affected the retinal pattern, signal intensities of nonneuronal extraocular muscle of diabetic WT mice and age-matched controls were compared. As expected, extraocular muscle signal intensity increased after manganese injection (data not shown). Extraocular muscle intensity of 1.5- to 4-month diabetic mice (73.9 ± 2.0 AU; $n = 16$) were not different ($P > 0.05$) from that of age-matched WT mice (73.1 ± 3.0 AU; $n = 12$).

Effect of SOD1 Overexpression—Diabetic Hilltop mice had subnormal ($P = 0.0001$) intraretinal manganese uptake compared with nondiabetic modified Hilltop mice. Compared with diabetic and nondiabetic modified Hilltop mice, which were age matched to the SOD1OE groups, nondiabetic and diabetic mice SOD1OE mice had normal inner and outer retinal signal intensities ($P > 0.05$; Fig. 3). Note that although they were not age matched, the same conclusions would have been drawn had Jackson mice been used in the analysis instead (data not shown).

Retinal Thickness—In control mice, whole retinal thickness (range, 195−230 μm) remained constant with aging ($r = 0.07$; $P = 0.75$), and the data were combined to produce a mean WT thickness of 211 ± 2 μm ($n = 21$). In diabetic mice a similar range of thickness was noted (183 −234 μm), and the mean thickness (209 ± 2 mm) was not different ($P > 0.05$) from control values. As diabetic mice aged, retinal thickness decreased (0.9 months of diabetes, 220 ± 3 μm [$n = 5$]; 1.5 months, 208 ± 7 μm [$n = 6$]; 2.5 months, 205 ± 2 μm [$n = 5$]; 5.5 months, 201 ± 2 μm [$n = 6$]; 7.4 months, 206 ± 5 μm [$n = 5$]) in a linear fashion (thickness = 216 − 2 × (duration of diabetes [months]); $r = -0.4$; $P = 0.02$). Nondiabetic 5-month-old SOD1OE mice had an average retinal thickness (197 ± 2 μm) different ($P < 0.05$) from that of age-matched control WT mice and 4.2-month-old diabetic SOD1OE mice (211 ± 3 μm).

Histopathology—In WT mice, 9 to 10 months of diabetes caused a significant increase ($P < 0.05$) in the number of degenerate retinal capillaries (Fig. 4). Nondiabetic SOD1OE mice had more degenerate capillaries than did WT nondiabetic mice ($P < 0.05$). Compared with age-matched nondiabetic SOD1OE mice, diabetes did not cause any further increase in capillary degeneration in SOD1OE mice ($P > 0.05$; Fig. 4).

Discussion

In this study, three major results were found. First, in WT mice, layer-specific MEMRI data correlated with normal physiology associated with light and dark visual processing. These results support and extend our previous work demonstrating similar intraretinal light/dark changes in the rat.[39] Second, in diabetic WT mice, we found a diabetes duration-dependent evolution in the uptake of manganese in photoreceptor and postreceptor retina. These associative observations are consistent with and broaden our earlier report in diabetic rats that reduced retinal manganese uptake occurred early and reflected a decrease in ion regulation within the retina.[17] Third, diabetic SOD1OE mice, unlike diabetic WT mice, had normal intraretinal manganese uptake. Nondiabetic SOD1OE mice experienced modest but significant retinal thinning and vascular degeneration, raising questions about the suitability of SOD1 overexpression as a means of inhibiting diabetic retinopathy. Nonetheless, the present results support the use of MEMRI in murine models as a powerful, objective, and noninvasive approach to measure early intraretinal ion dysregulation by, for example, oxidative stress.

The dose of $MnCl_2$ used in the present study (66 mg/kg) was not expected to adversely affect retinal function or anatomy. Previously, we established that a 33% lower dose of $MnCl_2$ (44 mg/kg) was not associated with changes in retinal function as assessed with ERG parameters at 4 hours or 7 days after injection compared with control rats.[35] In addition, at 30 days after injection, whole and inner retinal thickness, intraocular pressure, and blood retinal barrier permeability surface area product were not different from those of control rats.[39] However, in a preliminary study, the 44 mg/kg dose of $MnCl_2$ did not produce reliable contrast changes in the mouse retina, possibly because of the relatively higher overall metabolic rate in the mouse (data not shown). Instead, it was found empirically that a higher dose of manganese (66 mg/kg) produced more robust retinal contrast changes. This dose was similar to, or lower than, that used in other mouse MEMRI studies and was well below that needed to induce neurotoxicity.[34,49] The strongest possibility of future human application of MEMRI will likely involve an already FDA-approved manganese-based contrast agent (Teslascan; GE Healthcare, Chalfont, St. Giles, UK). However, in experimental studies, we sought to maximize the amount of manganese taken up by the retina to fully evaluate the potential usefulness of MEMRI; hence, we used $MnCl_2$ to maximize the dynamic range and sensitivity to subtle changes. Our preliminary results in rats (data not shown) demonstrated that intraretinal uptake of manganese can be robustly measured with MEMRI with a clinically relevant dose and route of manganese-based contrast agent (Teslascan; GE Healthcare). In any event, it was reasonable

to consider the 66-mg/kg dose as nontoxic and the intraretinal uptake of manganese as a quantitative biomarker of ion activity regulation in vivo.

In previous rat studies, MEMRI was validated in rats as providing an accurate measure of retinal thickness without choroidal contamination.[35,39] In this study, the mean MEMRI-measured retinal thickness from WT mice (195−230 μm) was similar to the range in the literature for mice (187−225 μm).[50–52] In addition, the MEMRI data were consistent with the expected whole retinal thinning that coincided with increasing duration of diabetes, as reported in other mouse studies.[6,17,50] Retinal thickness data from SOD1OE mice are discussed below. These considerations support the use of MEMRI as a spatially accurate approach for evaluating whole retinal thickness in rodents.

We have previously demonstrated that, in the rat, intraretinal manganese uptake patterns robustly correlate with normal retinal physiology responses associated with light and dark visual processing.[39] Normally, in dark-adapted retina, ion activity and demand in photoreceptors increases through the opening of cGMP-gated ion channels to generate the so-called dark current. In light-adapted retina, photoreceptors hyperpolarize in response to light by closure of the cGMP-gated ion channels by way of the phototransduction cascade. Thus, the activity and ion demand of photoreceptors are increased in the dark and attenuated in the light. The situation in the inner retina is more complex. When the retina is dark adapted, the OFF pathway (OFF bipolar cell to OFF ganglion cell) is active in the inner retina; conversely, in the light, the ON pathway (ON bipolar cell to ON ganglion cell) is depolarizing. With equal representation of ON and OFF cells (bipolar and ganglion cells) in the retina, changes in inner retina activity caused by light or dark adaptation would be expected to be relatively equal. The light/dark results reported here (Fig. 1) provide additional support for the use of MEMRI as a sensitive probe of normal retinal physiology.

Here, as in a previous report, control animals demonstrated relatively consistent intraretinal signal intensities for the duration of the study.[53] These data provide confidence in the reliability of the MEMRI examination. After 0.9 months of diabetes, no significant change in intraretinal ion regulation from control values was noted. These results are consistent with a lack of retinal toxicity of streptozotocin.[4] Between 1.5 and 4 months of diabetes, significant and sustained subnormal retinal uptake of manganese occurred that was reminiscent of previous findings of subnormal uptake measured between 3 and 4.5 months of diabetes in diabetic rat models.[17] The mechanism involved with this reduced retinal manganese uptake is not yet understood. One possible explanation is that the observed retinal ion dysregulation is secondary to diabetes-induced systemic changes in, for example, baseline plasma or tissue manganese levels. Clinically, baseline plasma levels of manganese are not different in patients with and without diabetes.[54,55] Experimentally, large decreases in plasma manganese concentrations with diabetes are not expected because, in diabetic rats, baseline manganese levels in retina and other tissues are not different from those in controls.[17,56] To further address this issue, we assumed that manganese uptake in muscle mirrored how each animal systemically handled manganese after intraperitoneal injection because muscle does not have a blood barrier. No differences in extraocular muscle manganese uptake were noted. When all these results are considered, we find no compelling evidence that systemic effects of diabetes contribute to the present observations.

Given that impaired retinal ion regulation between 1.5 and 4 months of diabetes preceded the onset of retinal cellular loss, it was unlikely to have been a consequence of degeneration. A likely alternative explanation for the subnormal uptake results in this study involves hyperglycemic increases in lipid peroxidation and protein glycation that could reduce the activity of major membrane-bound regulators of ion homeostasis (e.g., Na^+/K^+-ATPase, calcium ATPase, and ion exchangers) in retina.[12,32] Previously, we reported in control rats

that the inhibition of retinal Na^+/K^+-ATPase activity with ouabain resulted in subnormal intraretinal manganese uptake.[35]

At 5.5 and 7.4 months of diabetes, the extent of retinal manganese uptake significantly increased to normal levels compared with that at 1.5 to 4 months of diabetes. This relative increase was consistent with a previously identified pattern in two different nondiabetic models in which a similar relative elevation in intraretinal manganese uptake from subnormal levels occurred with vascular or neuronal degeneration.[53] We speculate that this subsequent increase in intraretinal manganese uptake indicated a gradual and abnormal opening of ion channels that eventually led to calcium overload, apoptosis, and vascular and neuronal cellular loss.[57] In diabetic retinopathy and in retinopathies with similarities to diabetic retinopathy, therapies that prevent this relative increase are strongly linked with neuroprotection and vasculoprotection.[17,35] In particular, in diabetic rodents, late development of vascular histopathology continues even if good glycemic control is reinitiated at 6 months of hyperglycemia, after the relative increase in intraretinal manganese uptake, but not if good control is started at 2 months of diabetes when manganese uptake is subnormal.[58] These considerations highlight the extent of intraretinal manganese uptake as a robust biomarker in emerging diabetic retinopathy.

In this study, intraretinal ion regulation of diabetic SOD1OE mice was evaluated only at a single point, raising the potential concern that subnormal uptake might have developed earlier or later than the measurement time point. We do not consider either possibility likely in light of strong link between the early intraretinal ionic dysregulatory pattern described with later retinal degeneration and the lack of evidence for diabetes-induced degeneration in the diabetic SOD1OE retina. Retinas from C57BL/6 mice can develop more capillary degeneration than was measured here in the diabetic SOD1OE mice.[59] Thus, it seems reasonable to postulate that diabetes had the potential to cause more vascular degeneration than was found in the present study. In addition, the diabetic SOD1OE uptake data are consistent with previous findings that α-lipoic acid treatment prevented early intraretinal ion dysregulation and later development of histopathology.[17]

In nondiabetic SOD1OE mice, we found modest neuronal (retinal thinning) and vascular (acellular capillaries) degeneration but normal intraretinal uptake of manganese. This pattern is consistent with the ionic dysregulatory pattern linked with degeneration. Nondiabetic SOD2 overexpressor mice do not display these morphometric abnormalities,[22] and the reason for this difference with the present SOD1OE data is unclear. One possible explanation for the presence of retinal neuronal and vascular degeneration might involve SOD1 overexpression resulting in increased production of hydrogen peroxide in the cytosol[41,60] compared with the level of activity of its detoxification enzyme catalase. Several studies have hypothesized that nondiabetic SOD1OE mice demonstrate reduced retinal neuronal and vascular anatomic damage after various types of injury,[27–29] yet support for this hypothesis has been ambiguous.[27–29] Notably, Levkovitch-Verbin et al.[27] found that SOD1OE mice experience exacerbated retinal ganglion cell death after optic nerve injury.

In conclusion, the potential benefit of SOD1 overexpression to inhibit retinal abnormalities in this model is limited by the retinal and vascular degeneration that develops independently of diabetes. Nonetheless, MEMRI was shown to be sensitive to physiological changes in intraretinal ion regulation in mice. Our data in diabetic rodents support a key role of increased oxidative stress in general, and superoxide ion in particular, in the diabetes-induced reduction in intraretinal manganese uptake.[17] Intriguingly, we identified distinct time periods during which intraretinal manganese uptake was subnormal (1.5−4 months of diabetes) and was followed by a relative increase (>5.5 months of diabetes). These periods corresponded well with previously reported temporal windows when intervention with insulin therapy either was

(2 months of diabetes) or was not (6 months of diabetes) successful at inhibiting later histopathology.[58] These considerations, and those of other studies,[53] raise the possibility that though subnormal intraretinal uptake is an ominous development in emerging diabetic retinopathy, intervention is more likely to be successful during this time than after the subsequent relative increase.

Acknowledgments

Supported by National Institutes of Health Grants EY010221 (BAB) and EY00300 (TSK); Juvenile Diabetes Research Foundation (BAB); National Institutes of Health Animal Models of Diabetic Complications Consortium and Mouse Metabolic Phenotyping Centers Pilot and Feasibility Programs (BAB); and an unrestricted grant from Research to Prevent Blindness (Kresge Eye Institute).

References

1. Grunwald JE, Riva CE, Brucker AJ, Sinclair SH, Petrig BL. Altered retinal vascular response to 100% oxygen breathing in diabetes mellitus. Ophthalmology 1984;91(12):1447–1452. [PubMed: 6084214]
2. Sinclair SH, Grunwald JE, Riva CE, Braunstein SN, Nichols CW, Schwartz SS. Retinal vascular autoregulation in diabetes mellitus. Ophthalmology 1982;89(7):748–750. [PubMed: 7122050]
3. Trick GL, Berkowitz BA. Retinal oxygenation response and retinopathy. Prog Retin Eye Res 2005;24 (2):259–274. [PubMed: 15610976]
4. Phipps JA, Fletcher EL, Vingrys AJ. Paired-flash identification of rod and cone dysfunction in the diabetic rat. Invest Ophthalmol Vis Sci 2004;45(12):4592–4600. [PubMed: 15557472]
5. Han Y, Bearse MA Jr, Schneck ME, Barez S, Jacobsen CH, Adams AJ. Multifocal electroretinogram delays predict sites of subsequent diabetic retinopathy. Invest Ophthalmol Vis Sci 2004;45(3):948–954. [PubMed: 14985316]
6. Barber AJ, Lieth E, Khin SA, Antonetti DA, Buchanan AG, Gardner TW. Neural apoptosis in the retina during experimental and human diabetes: early onset and effect of insulin. J Clin Invest 1998;102 (4):783–791. [PubMed: 9710447]
7. Schaefer S, Kajimura M, Tsuyama S, et al. Aberrant utilization of nitric oxide and regulation of soluble guanylate cyclase in rat diabetic retinopathy. Antioxid Redox Signal 2003;5(4):457–465. [PubMed: 13678534]
8. Barber AJ, Antonetti DA, Kern TS, et al. The Ins2Akita mouse as a model of early retinal complications in diabetes. Invest Ophthalmol Vis Sci 2005;46(6):2210–2218. [PubMed: 15914643]
9. Barber AJ. A new view of diabetic retinopathy: a neurodegenerative disease of the eye. Prog Neuropsychopharmacol Biol Psychiatry 2003;27(2):283–290. [PubMed: 12657367]
10. Budzynski E, Wangsa-Wirawan N, Padnick-Silver L, Hatchell D, Linsenmeier R. Intraretinal pH in diabetic cats. Curr Eye Res 2005;30(3):229–240. [PubMed: 15804749]
11. Ottlecz A, Bensaoula T, Eichberg J, Peterson RG. Angiotensin-converting enzyme activity in retinas of streptozotocin-induced and Zucker diabetic rats: the effect of angiotensin II on Na+,K(+)-ATPase activity. Invest Ophthalmol Vis Sci 1996;37(11):2157–2164. [PubMed: 8843902]
12. Kern TS, Kowluru RA, Engerman RL. Abnormalities of retinal metabolism in diabetes or galactosemia: ATPases and glutathione. Invest Ophthalmol Vis Sci 1994;35(7):2962–2967. [PubMed: 8206713]
13. Ottlecz A, Garcia CA, Eichberg J, Fox DA. Alterations in retinal Na+, K(+)-ATPase in diabetes: streptozotocin-induced and Zucker diabetic fatty rats. Curr Eye Res 1993;12(12):1111–1121. [PubMed: 8137634]
14. MacGregor LC, Matschinsky FM. Altered retinal metabolism in diabetes, II: measurement of sodium-potassium ATPase and total sodium and potassium in individual retinal layers. J Biol Chem 1986;261 (9):4052–4058. [PubMed: 3005315]
15. Zhang P, Hatter A, Liu B. Manganese chloride stimulates rat microglia to release hydrogen peroxide. Toxicol Lett 2007;173(2):88–100. [PubMed: 17669604]

16. Di Leo MA, Santini SA, Cercone S, et al. Chronic taurine supplementation ameliorates oxidative stress and Na^+ K^+ ATPase impairment in the retina of diabetic rats. Amino Acids 2002;23(4):401–406. [PubMed: 12436207]

17. Berkowitz BA, Roberts R, Stemmler A, Luan H, Gradianu M. Impaired apparent ion demand in experimental diabetic retinopathy: correction by lipoic acid. Invest Ophthalmol Vis Sci 2007;48(10): 4753–4758. [PubMed: 17898301]

18. Ottlecz A, Bensaoula T. Captopril ameliorates the decreased Na+,K(+)-ATPase activity in the retina of streptozotocin-induced diabetic rats. Invest Ophthalmol Vis Sci 1996;37(8):1633–1641. [PubMed: 8675407]

19. Zhang JZ, Xi X, Gao L, Kern TS. Captopril inhibits capillary degeneration in the early stages of diabetic retinopathy. Curr Eye Res 2007;32(10):883–889. [PubMed: 17963108]

20. Kowluru RA, Atasi L, Ho YS. Role of mitochondrial superoxide dismutase in the development of diabetic retinopathy. Invest Ophthalmol Vis Sci 2006;47(4):1594–1599. [PubMed: 16565397]

21. Sadi G, Yilmaz O, Guray T. Effect of vitamin C and lipoic acid on streptozotocin-induced diabetes gene expression: mRNA and protein expressions of Cu-Zn SOD and catalase. Mol Cell Biochem 2008;309(1–2):109–116. [PubMed: 18008141]

22. Kanwar M, Chan PS, Kern TS, Kowluru RA. Oxidative damage in the retinal mitochondria of diabetic mice: possible protection by superoxide dismutase. Invest Ophthalmol Vis Sci 2007;48(8):3805–3811. [PubMed: 17652755]

23. Kowluru RA, Kowluru V, Xiong Y, Ho YS. Overexpression of mitochondrial superoxide dismutase in mice protects the retina from diabetes-induced oxidative stress. Free Radic Biol Med 2006;41(8): 1191–1196. [PubMed: 17015165]

24. Marklund SL. Extracellular superoxide dismutase and other superoxide dismutase isoenzymes in tissues from nine mammalian species. Biochem J 1984;222(3):649–655. [PubMed: 6487268]

25. Behndig A, Svensson B, Marklund SL, Karlsson K. Superoxide dismutase isoenzymes in the human eye. Invest Ophthalmol Vis Sci 1998;39(3):471–475. [PubMed: 9501855]

26. Okado-Matsumoto A, Fridovich I. Subcellular distribution of superoxide dismutases (SOD) in rat liver. Cu,Zn-SOD in mitochondria. J Biol Chem 2001;276(42):38388–38393. [PubMed: 11507097]

27. Levkovitch-Verbin H, Harris-Cerruti C, Groner Y, Wheeler LA, Schwartz M, Yoles E. RGC death in mice after optic nerve crush injury: oxidative stress and neuroprotection. Invest Ophthalmol Vis Sci 2000;41(13):4169–4174. [PubMed: 11095611]

28. Klaeger C, de Sa L, Klaeger AJ, Carlson EJ, Good WV, Epstein CJ. An elevated level of copper zinc superoxide dismutase fails to prevent oxygen induced retinopathy in mice. Br J Ophthalmol 1996;80 (5):429–434. [PubMed: 8695565]

29. Dong A, Shen J, Krause M, et al. Superoxide dismutase 1 protects retinal cells from oxidative damage. J Cell Physiol 2006;208(3):516–526. [PubMed: 16741961]

30. Kowluru RA, Kern TS, Engerman RL. Abnormalities of retinal metabolism in diabetes or experimental galactosemia, IV: antioxidant defense system. Free Radic Biol Med 1997;22(4):587–592. [PubMed: 9013121]

31. Kowluru RA, Kern TS, Engerman RL, Armstrong D. Abnormalities of retinal metabolism in diabetes or experimental galactosemia, III: effects of antioxidants. Diabetes 1996;45(9):1233–1237. [PubMed: 8772728]

32. Kowluru R. Retinal metabolic abnormalities in diabetic mouse: comparison with diabetic rat. Curr Eye Res 2002;24(2):123–128. [PubMed: 12187484]

33. Lin YJ, Koretsky AP. Manganese ion enhances T1-weighted MRI during brain activation: an approach to direct imaging of brain function. Magn Reson Med 1997;38(3):378–388. [PubMed: 9339438]

34. Yu X, Wadghiri YZ, Sanes DH, Turnbull DH. In vivo auditory brain mapping in mice with Mn-enhanced MRI. Nat Neurosci 2005;8(7):961–968. [PubMed: 15924136]

35. Berkowitz BA, Roberts R, Luan H, et al. Manganese-enhanced MRI studies of alterations of intraretinal ion demand in models of ocular injury. Invest Ophthalmol Vis Sci 2007;48(8):3796–3804. [PubMed: 17652754]

36. Berkowitz BA, Roberts R, Penn JS, Gradianu M. High-resolution manganese-enhanced MRI of experimental retinopathy of prematurity. Invest Ophthalmol Vis Sci 2007;48(10):4733–4740. [PubMed: 17898298]

37. Braun RD, Gradianu M, Vistisen KS, Roberts RL, Berkowitz BA. Manganese-enhanced MRI of human choroidal melanoma xenografts. Invest Ophthalmol Vis Sci 2007;48(3):963–967. [PubMed: 17325133]
38. Wendland MF. Applications of manganese-enhanced magnetic resonance imaging (MEMRI) to imaging of the heart. NMR Biomed 2004;17(8):581–594. [PubMed: 15761947]
39. Berkowitz BA, Roberts R, Goebel DJ, Luan H. Noninvasive and simultaneous imaging of layer-specific retinal functional adaptation by manganese-enhanced MRI. Invest Ophthalmol Vis Sci 2006;47(6):2668–2674. [PubMed: 16723485]
40. Lu H, Xi ZX, Gitajn L, Rea W, Yang Y, Stein EA. Cocaine-induced brain activation detected by dynamic manganese-enhanced magnetic resonance imaging (MEMRI). Proc Natl Acad Sci U S A 2007;104(7):2489–2494. [PubMed: 17287361]
41. Craven PA, Melhem MF, Phillips SL, DeRubertis FR. Overexpression of $Cu2^{+}/Zn2^{+}$ superoxide dismutase protects against early diabetic glomerular injury in transgenic mice. Diabetes 2001;50(9): 2114–2125. [PubMed: 11522679]
42. Epstein CJ, Avraham KB, Lovett M, et al. Transgenic mice with increased Cu/Zn-superoxide dismutase activity: animal model of dosage effects in Down syndrome. Proc Natl Acad Sci U S A 1987;84(22):8044–8048. [PubMed: 2960971]
43. Schupp DG, Merkle H, Ellermann JM, Ke Y, Garwood M. Localized detection of glioma glycolysis using edited 1H MRS. Magn Reson Med 1993;30(1):18–27. [PubMed: 8371670]
44. Kern TS, Engerman RL. Pharmacological inhibition of diabetic retinopathy: aminoguanidine and aspirin. Diabetes 2001;50(7):1636–1642. [PubMed: 11423486]
45. Zheng L, Szabo C, Kern TS. Poly(ADP-ribose) polymerase is involved in the development of diabetic retinopathy via regulation of nuclear factor-κB. Diabetes 2004;53(11):2960–2967. [PubMed: 15504977]
46. Berkowitz BA. Adult and newborn rat inner retinal oxygenation during carbogen and 100% oxygen breathing: comparison using magnetic resonance imaging delta PO_2 mapping. Invest Ophthalmol Vis Sci 1996;37(10):2089–2098. [PubMed: 8814148]
47. Cheng H, Nair G, Walker TA, et al. Structural and functional MRI reveals multiple retinal layers. Proc Natl Acad Sci U S A 2006;103(46):17525–17530. [PubMed: 17088544]
48. Liang Z. Longitudinal data analysis using generalized linear models. Biometrika 1986;73:13–22.
49. Silva AC, Lee JH, Aoki I, Koretsky AP. Manganese-enhanced magnetic resonance imaging (MEMRI): methodological and practical considerations. NMR Biomed 2004;17(8):532–543. [PubMed: 15617052]
50. Martin PM, Roon P, Van Ells TK, Ganapathy V, Smith SB. Death of retinal neurons in streptozotocin-induced diabetic mice. Invest Ophthalmol Vis Sci 2004;45(9):3330–3336. [PubMed: 15326158]
51. Zhou X, Xie J, Shen M, et al. Biometric measurement of the mouse eye using optical coherence tomography with focal plane advancement. Vision Res 2008;48(9):1137–1143. [PubMed: 18346775]
52. Remtulla S, Hallett PE. A schematic eye for the mouse, and comparisons with the rat. Vision Res 1985;25(1):21–31. [PubMed: 3984214]
53. Berkowitz BA, Gradianu M, Schafer S, et al. Ionic dysregulatory phenotyping of pathologic retinal thinning with manganese-enhanced MRI. Invest Ophthalmol Vis Sci 2008;49:3178–3184. [PubMed: 18362105]
54. Cooper GJS, Chan YK, Dissanayake AM, et al. Demonstration of a hyperglycemia-driven pathogenic abnormality of copper homeostasis in diabetes and its reversibility by selective chelation: quantitative comparisons between the biology of copper and eight other nutritionally essential elements in normal and diabetic individuals. Diabetes 2005;54(5):1468–1476. [PubMed: 15855335]
55. Walter RM Jr, Uriu-Hare JY, Olin KL, et al. Copper, zinc, manganese, and magnesium status and complications of diabetes mellitus. Diabetes Care 1991;14(11):1050–1056. [PubMed: 1797486]
56. Failla ML, Kiser RA. Altered tissue content and cytosol distribution of trace metals in experimental diabetes. J Nutr 1981;111(11):1900–1909. [PubMed: 7028924]
57. Osborne NN, Casson RJ, Wood JP, Chidlow G, Graham M, Melena J. Retinal ischemia: mechanisms of damage and potential therapeutic strategies. Prog Retin Eye Res 2004;23(1):91–147. [PubMed: 14766318]

58. Kowluru RA, Kanwar M, Kennedy A. Metabolic memory phenomenon and accumulation of peroxynitrite in retinal capillaries. Exp Diabetes Res 2007;2007:21976. [PubMed: 17641740]

59. Kern TS, Engerman RL. A mouse model of diabetic retinopathy. Arch Ophthalmol 1996;114(8):986–990. [PubMed: 8694735]

60. DeRubertis FR, Craven PA, Melhem MF, Salah EM. Attenuation of renal injury in db/db mice overexpressing superoxide dismutase: evidence for reduced superoxide-nitric oxide interaction. Diabetes 2004;53(3):762–768. [PubMed: 14988262]

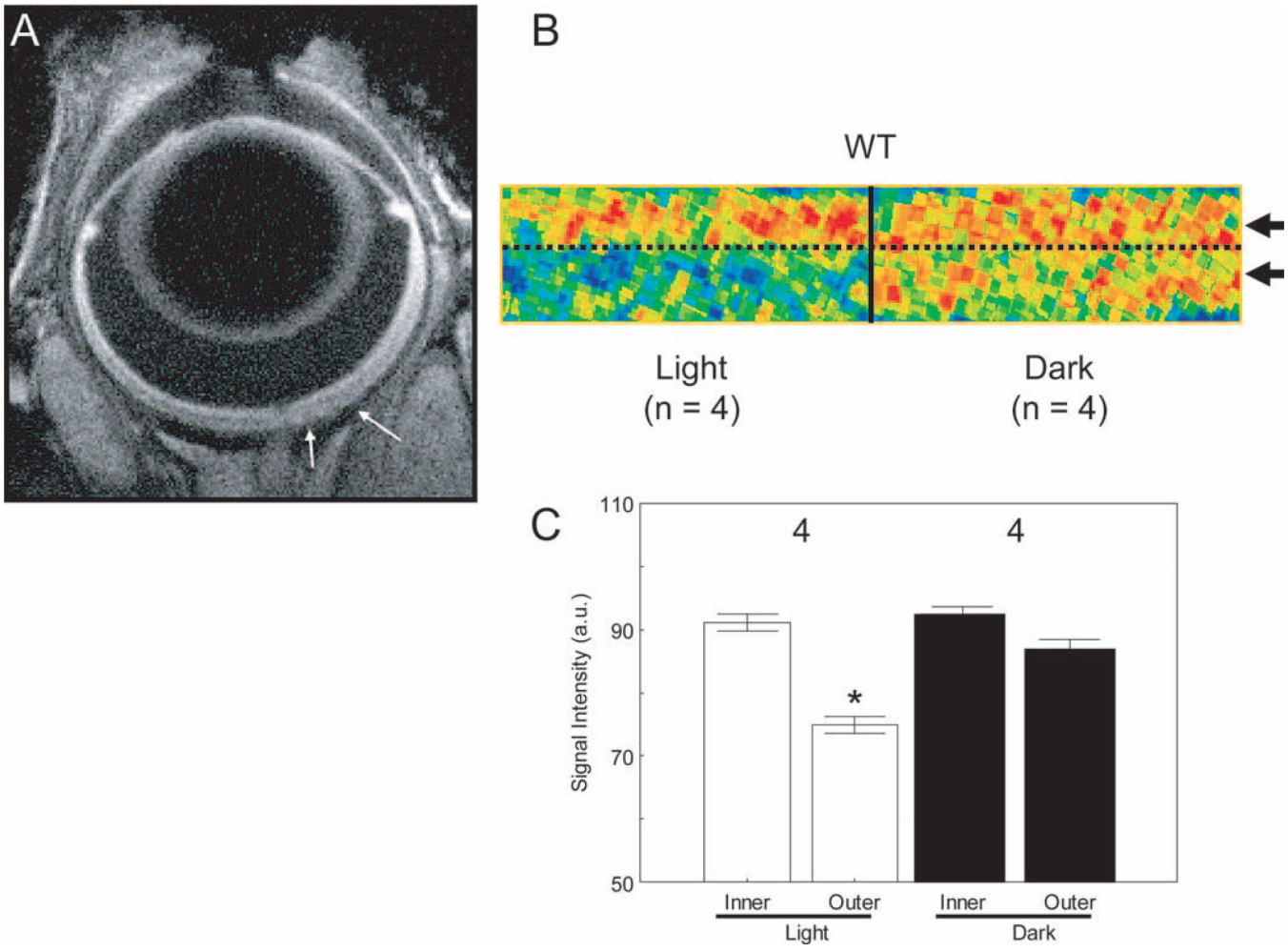

Figure 1.

MEMRI changes in murine inner and outer retinal signal intensity with light and dark adaptation. (**A**) Representative MEMRI of a WT mouse eye. *White arrows*: region illustrated in (**B**). (**B**) Pseudocolor-linearized images of average retinal signal intensity in central retina of WT mice (*left*, light adapted, $n = 4$; *right*, dark adapted, $n = 4$). The same pseudocolor scale was used for linearized images in which *blue* to *green* to *yellow* to *red* represent lowest to highest signal intensity. *Dotted black line*: boundary between inner and outer retina, as demonstrated in previous studies.[39] Intraretinal locations from which inner retinal (IR) and outer retinal (OR) data were extracted and used in this study are indicated by the *black arrows* on the *right* of the dark-adapted linearized image. (**C**) Summary of IR and OR signal intensities in light- and dark-adapted mice. Numbers of animals used to generate these data are listed above each bar. Error bars represent the SEM. Comparisons were performed between inner retinal signal intensities during light or dark adaptation and between outer retina values during the different adaptation conditions. *$P = 0.0025$. The *y*-axis scale starts at 50 because this is the pre–manganese baseline level determined from uninjected mice (data not shown).

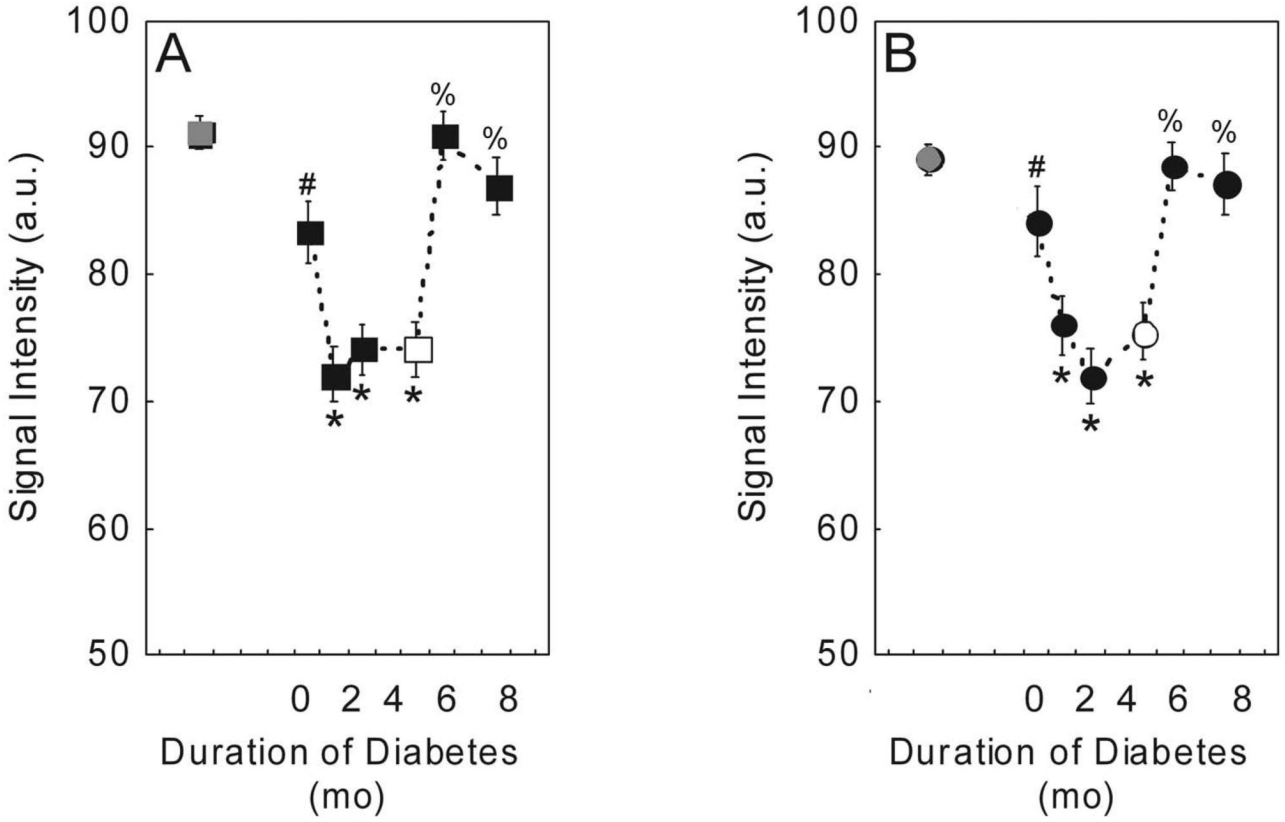

Figure 2.

Summary of natural history of signal intensities for (**A**) inner retina (IR) and (**B**) outer retina (OR). *Gray symbols*: average WT (combined Jackson and modified Hilltop mice) IR and OR intensities. **P* = 0.0001 for 1.5, 2.5, and 4 months of diabetes, 2-tailed, compared with average WT IR (91.0 ± 0.6 AU; *n* = 21) or OR (89.1 ± 0.6 AU) intensities. $^{\%}P$ = 0.0001 (5.5 and 7.4 months of diabetes); $^{\#}P$ = 0.02 (IR) or 0.05 (OR) (0.9 months of diabetes), 2-tailed, compared with average IR (75.8 ± 0.6 AU; *n* = 21) or OR (76.6 ± 0.6 AU) of mice with 1.5 to 4 months of diabetes. *White symbols*: modified 4-month-old diabetic Hilltop mice signal intensities are shown for clarity. Error bars are SEM. The *y*-axis scale starts at 50 because this is the pre–manganese baseline level determined from uninjected mice (data not shown).

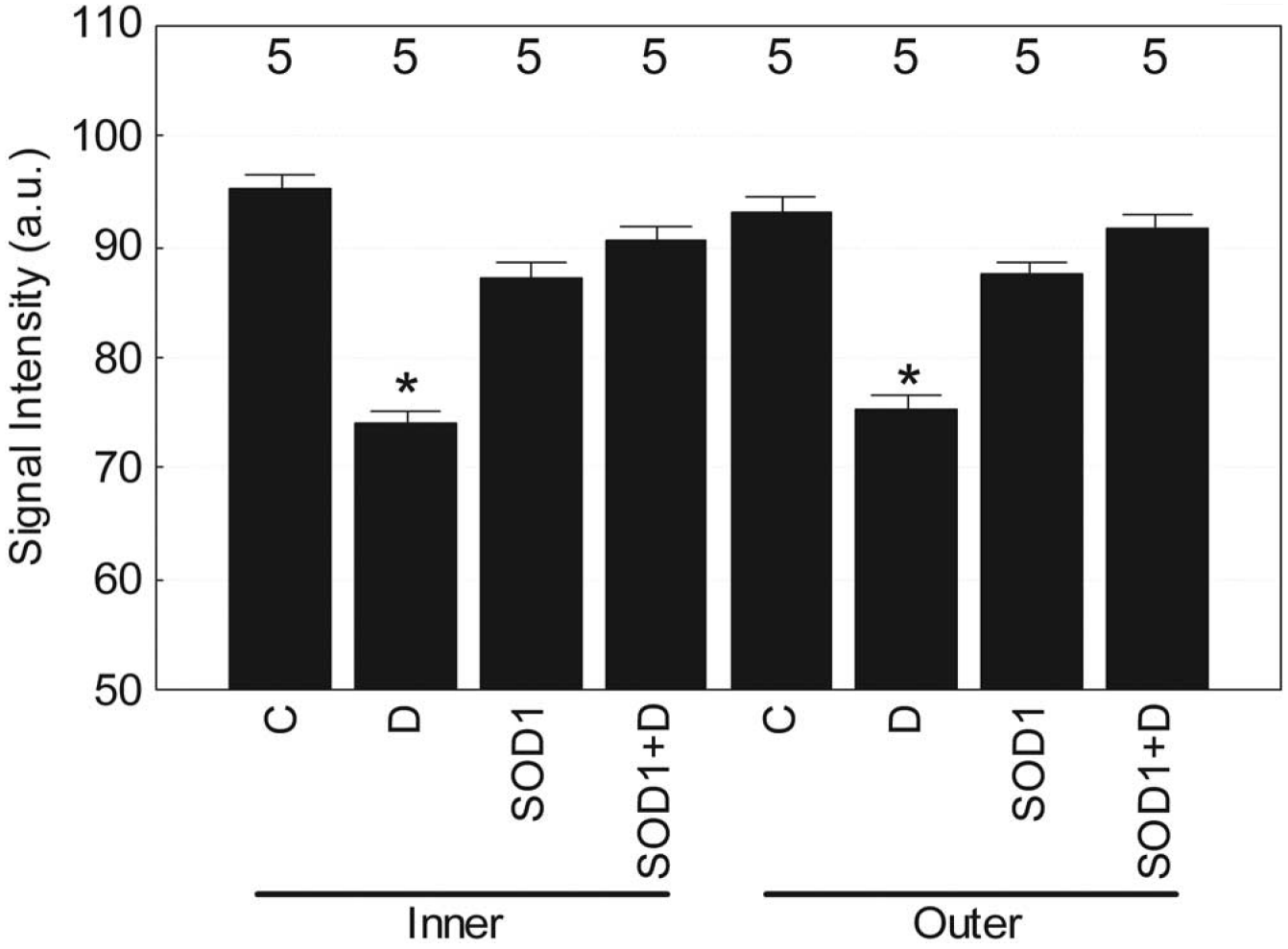

Figure 3.

Summary of changes in mean MEMRI intraretinal signal intensity in control and diabetic WT and SOD1OE mice. The *y*-axis scale starts at 50 because this is the pre–manganese baseline level determined from uninjected mice (data not shown). *Asterisk*: signifi-cant comparisons with control inner and outer retina intensities are shown ($P = 0.0001$). Error bars are SEM, and numbers over bars are numbers of animals studied.

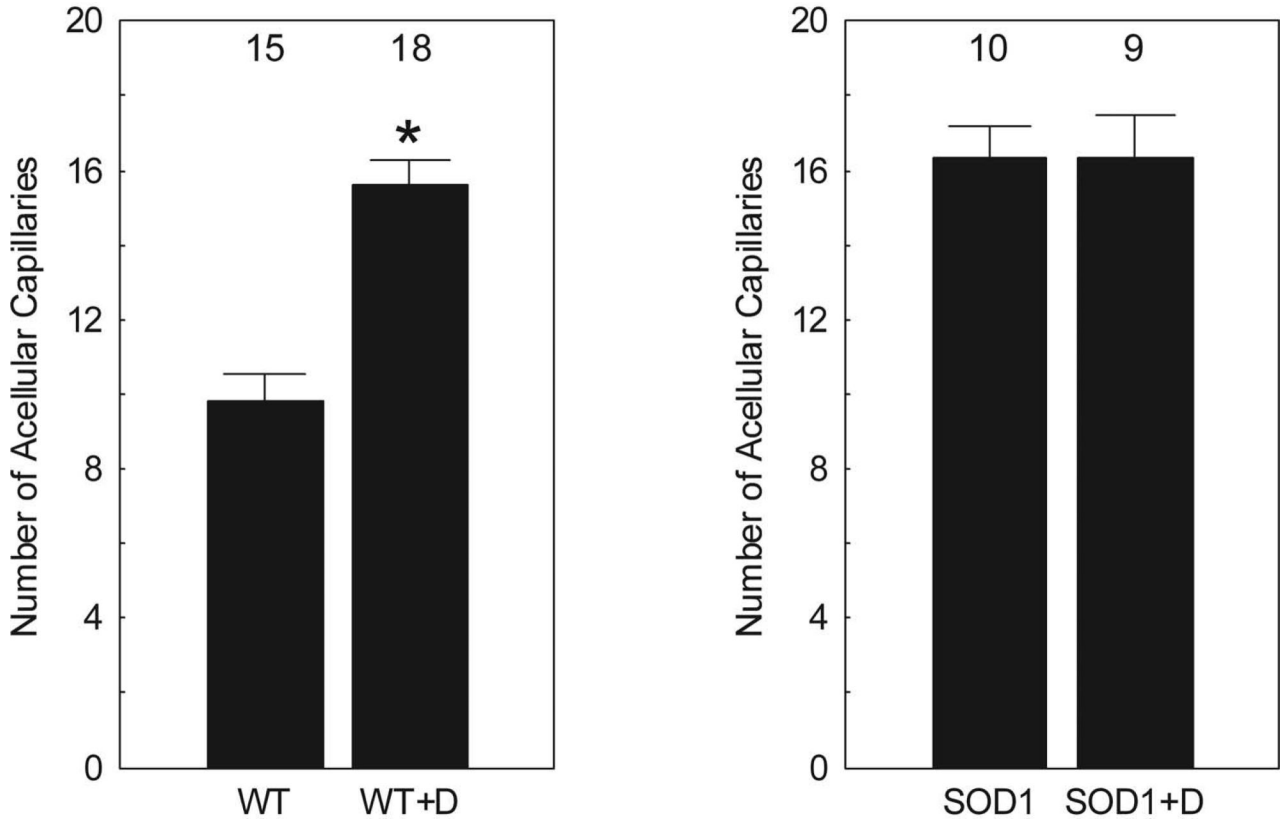

Figure 4.

Plot of number of mean degenerate retinal capillaries (acellular capillaries) in diabetic WT mice (9 months of study; WT+D) compared with that in nondiabetic controls (WT; *left*) and diabetic SOD1OE mice (SOD1+D) compared with that in nondiabetic SOD1OE controls (SOD1; *right*). Diabetes-induced capillary degeneration was increased in WT (WT+D) but not SOD1 overexpressor (SOD1+D) mice. Numbers of animals used to generate these data are listed above each bar. Error bars represent the SEM. *$P < 0.05$ was considered significant.